Hindawi Publishing Corporation
Mathematical Problems in Engineering
Volume 2011, Article ID 793798, 21 pages
doi:10.1155/2011/793798

Research Article

The Nonlinear Instability Modes of Dished Shallow Shells under Circular Line Loads

Liu Chang-Jiang,[1,2] Zheng Zhou-Lian,[1,2,3] Huang Cong-Bing,[1,2,4] He Xiao-Ting,[1,2] Sun Jun-Yi,[1,2] and Chen Shan-Lin[1,2]

[1] *College of Civil Engineering, Chongqing University, Chongqing 400045, China*
[2] *Key Laboratory of New Technology for Construction of Cities in Mountain Area (Chongqing University), Ministry of Education, Chongqing 400045, China*
[3] *Chongqing Vocational College of Architectral Engineering, Chongqing 400039, China*
[4] *Internal Trade Engineering and Research Institute, Beijing 100069, China*

Correspondence should be addressed to Liu Chang-Jiang, changjiangliucd@126.com and Zheng Zhou-Lian, zhengzhoulian@yahoo.com.cn

Received 17 August 2010; Revised 14 February 2011; Accepted 15 February 2011

Academic Editor: E. E. N. Macau

This paper investigated the nonlinear stability problem of dished shallow shells under circular line loads. We derived the dimensionless governing differential equations of dished shallow shell under circular line loads according to the nonlinear theory of plates and shells and solved the governing differential equations by combing the free-parameter perturbation method (FPPM) with spline function method (SFM) to analyze the nonlinear instability modes of dished shallow shell under circular line loads. By analyzing the nonlinear instability modes and combining with concrete computational examples, we obtained the variation rules of the maximum deflection area of initial instability with different geometric parameters and loading action positions and discussed the relationship between the initial instability area and the maximum deflection area of initial instability. The results obtained from this paper provide some theoretical basis for engineering design and instability prediction and control of shallow-shell structures.

1. Introduction

The dished shallow shell is a thin shallow shell that is composed by circular plate and shallow conical shell. The instability phenomenon of dished shallow shell is usually regarded as a control signal in automatic control systems of instruments. So, the theoretical analysis of nonlinear instability characters of dished shallow shell is necessary for the engineering design and application. The nonlinear stability problem of shallow shell has been focused and studied by many scholars, and some research results have been achieved. Liu and Chen [1, 2] applied the modified iteration method to study the nonlinear stability problem of

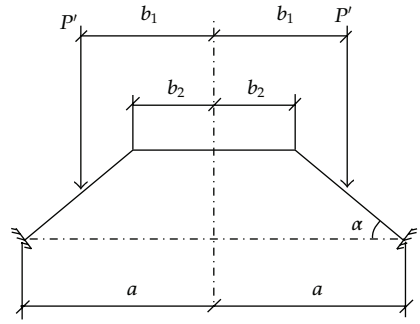

Figure 1: Geometrical size and load of the dished shallow shell.

dished shallow shells. Chakrabarti et al. [3] investigated the nonlinear stability of a shallow unsymmetrical heated orthotropic sandwich shell of double curvature with orthotropic core. Tani [4] studied the large deflection instability problem of truncated conical shells under compound loads by using finite difference method. Xu et al. [5] studied the nonlinear stability problem of truncated conical shell with variable thickness under uniformly distributed loads by applying modified iteration method. Ramsey [6] and H. Wang and J.-K. Wang [7] applied perturbation method to investigate the plastic instability problem of conical shells under axial pressure and the nonlinear instability problem of thin shallow conical shell under uniformly distributed loads. The existing research mainly focused on the characteristic equation that was constructed by the external load and the center deflection. The reason for the fact that they choose the center deflection to construct the characteristic equation is that they believe the instability characteristics firstly appear at the center point of the shallow shell, and they can discuss the overall stability according to this characteristic equation. Very few people discussed the nonlinear local stability problem of shallow shell, which is where does the shallow shell under external loads start to lose stability? (i.e., where is the initial instability area?). Only Zheng and Chen [8, 9] have studied the nonlinear local stability of dished shallow shell. However, so far, researchers have not presented studies of nonlinear instability modes of dished shallow shell or investigated the internal relationship between the initial instability area and the instability modes.

In this paper, the free-parameter perturbation method [10] and spline function method [11] are combined to analyze the nonlinear instability modes of dished shallow shell under circular line loads. The relationships between the maximum deflection area of initial instability and the geometrical parameter and loading position are studied when the simply supported dished shallow shell start to lose stability, and the internal relationships between the initial instability area and the initial instability modes are investigated. The research results obtain some valuable and significant conclusions for engineering application and theoretical research and provide some basis for engineering design and instability prediction and control.

2. Dimensionless Basic Equations

The dished shallow shell is shown in Figure 1. The radius of the bottom circular plate plane is a, the radius of the upper circular plate is b_2, the thickness of the dished shallow shell is h, and the radius of axisymmetric circular line load is b_1.

Choose the dimensionless quantities as follows:

$$W = \frac{w}{h} \cdot \sqrt{12 \cdot (1 - \nu^2)}, \qquad k = \sqrt{12 \cdot (1 - \nu^2)} \cdot \frac{f}{h}, \qquad \gamma' = \frac{b_1}{a}, \qquad \gamma = \frac{b_2}{a}, \qquad \theta = \frac{dW}{d\rho},$$
$$S = -\frac{a^2 \cdot \rho \cdot N_r}{E \cdot h^3} \cdot 12 \cdot \left(1 - \nu^2\right), \qquad \rho = \frac{r}{a}, \qquad P = \frac{a^2 \cdot b_2 \cdot P'}{E \cdot h^4} \cdot 12\left(1 - \nu^2\right) \cdot \sqrt{3(1 - \nu^2)}, \tag{2.1}$$

where w denotes deflection, E denotes Young's modulus, N_r denotes radial membrane force, r denotes radial coordinate value, v denotes Poisson's ratio, P' is load parameter, and f denotes the vector height of dished shallow shell: $f = a \cdot \mathrm{tg}\alpha$.

Introducing Heaviside step function:

$$u(\rho - \gamma) = \begin{cases} 1 & (\rho \geq \gamma), \\ 0 & (\rho < \gamma). \end{cases} \tag{2.2}$$

The dimensionless governing differential equations of the dished shallow shells under circular line loads [1] are

$$L(\rho\theta) = P \cdot \rho^2 - S \cdot [k \cdot u(\rho - \gamma) + \theta],$$
$$L(\rho S) = k \cdot \theta \cdot u(\rho - \gamma) + \frac{1}{2}\theta^2, \tag{2.3}$$

where $L(\cdots) = \rho \cdot (d/d\rho) \cdot (1/\rho) \cdot (d/d\rho)(\cdots)$.

The corresponding boundary conditions are

$$\rho = 0: \ \theta = 0, \qquad S = 0,$$
$$\rho = 1: \ \frac{d\theta}{d\rho} + \nu_1 \cdot \theta = 0, \qquad \frac{dS}{d\rho} - \nu_2 \cdot S = 0, \tag{2.4}$$

where the values of v_1 and v_2 are related to the concrete boundary conditions, and for the general boundary conditions, their values are as follows [10]:

rigidly clamped edge: $\nu_1 = \infty, \nu_2 = \nu$,
clamped but free slip edge: $\nu_1 = \infty, \nu_2 = \infty$,
simply supported but free slip edge: $\nu_1 = \nu, \nu_2 = \infty$,
simply supported: $\nu_1 = \nu, \nu_2 = \nu$.

3. The Free-Parameter Perturbation Expansion of Dimensionless Equation

Expand the dimensionless load P, angle θ, and radial membrane force S as the following forms with respect to the perturbation parameter ε:

$$P = P_1\varepsilon + P_2\varepsilon^2 + P_3\varepsilon^3 + \cdots + P_n\varepsilon^n + o\left(\varepsilon^{n+1}\right), \tag{3.1}$$

$$\theta = \theta_1\varepsilon + \theta_2\varepsilon^2 + \theta_3\varepsilon^3 + \cdots + \theta_n\varepsilon^n + o\left(\varepsilon^{n+1}\right), \tag{3.2}$$

$$S = S_1\varepsilon + S_2\varepsilon^2 + S_3\varepsilon^3 + \cdots + S_n\varepsilon^n + o\left(\varepsilon^{n+1}\right), \tag{3.3}$$

where P_i $(i = 1, 2, \ldots, n)$ are undetermined constant coefficients and θ_i and S_i $(i = 1, 2, \ldots, n)$ are undetermined coefficients with respect to ρ.

Substituting (3.1)–(3.3) into (2.3) and (2.4) and comparing the coefficient of the same order power of ε, we can obtain the following stepwise approximate equations:

when the coefficients of ε^1 are equal,

$$\begin{aligned} L(\rho\theta_1) &= P_1 \cdot F(\rho) - S_1 \cdot k \cdot u(\rho - \gamma), \\ L(\rho S_1) &= \theta_1 \cdot k \cdot u(\rho - \gamma), \end{aligned} \tag{3.4}$$

when the coefficients of ε^2 are equal,

$$\begin{aligned} L(\rho\theta_2) &= P_2 \cdot F(\rho) - S_2 \cdot k \cdot u(\rho - \gamma) - S_1 \cdot \theta_1, \\ L(\rho S_2) &= \theta_2 \cdot k \cdot u(\rho - \gamma) + \frac{1}{2} \cdot \theta_1^2, \end{aligned} \tag{3.5}$$

when the coefficients of ε^3 are equal,

$$\begin{aligned} L(\rho\theta_3) &= P_3 \cdot F(\rho) - S_3 \cdot k \cdot u(\rho - \gamma) - (S_1 \cdot \theta_2 + S_2 \cdot \theta_1), \\ L(\rho S_3) &= \theta_3 \cdot k \cdot u(\rho - \gamma) + \theta_1 \cdot \theta_2. \end{aligned} \tag{3.6}$$

According to the above derivation method, the four and more than four order power stepwise approximate equations can be obtained, but they will not be discussed here.

The corresponding boundary conditions for (3.4)–(3.6) can be expressed as follows:

$$\begin{aligned} &\rho = 0: \ \theta_i = 0, \qquad S_i = 0, \\ &\rho = 1: \ \frac{d\theta_i}{d\rho} + \nu_1 \cdot \theta_i = 0, \qquad \frac{dS_i}{d\rho} - \nu_2 \cdot S_i = 0, \end{aligned} \tag{3.7}$$

where $i = 1, 2, 3$.

Assume that $\varphi_i(\rho)$ and $\psi_i(\rho)$ are the functions that satisfy the following equations:

$$\begin{aligned} L(\rho\varphi_1) &= \rho^2 - k\cdot u(\rho-\gamma)\cdot\psi_1, \\ L(\rho\psi_1) &= k\cdot u(\rho-\gamma)\cdot\varphi_1, \end{aligned} \tag{3.8}$$

$$\begin{aligned} L(\rho\varphi_2) &= -k\cdot u(\rho-\gamma)\cdot\psi_2 - \psi_1\cdot\varphi_1, \\ L(\rho\psi_2) &= k\cdot u(\rho-\gamma)\cdot\varphi_2 + \frac{\varphi_1^2}{2}, \end{aligned} \tag{3.9}$$

$$\begin{aligned} L(\rho\varphi_3) &= -k\cdot u(\rho-\gamma)\cdot\psi_3 - (\psi_1\cdot\varphi_2 + \psi_2\cdot\varphi_1), \\ L(\rho\psi_1) &= k\cdot u(\rho-\gamma)\cdot\varphi_3 + \varphi_1\cdot\varphi_2, \end{aligned} \tag{3.10}$$

$\varphi_i(\rho)$ and $\psi_i(\rho)$ satisfy the following boundary conditions:

$$\begin{aligned} &\rho = 0: \ \varphi_i = 0, \qquad \psi_i = 0, \\ &\rho = 1: \ \frac{d\varphi_i}{d\rho} + \nu_1\cdot\varphi_i = 0, \qquad \frac{d\psi_i}{d\rho} - \nu_2\cdot\psi_i = 0, \end{aligned} \tag{3.11}$$

where $i = 1, 2, 3$.

We can prove the following formulas are correct according to (3.8)–(3.11):

$$\begin{aligned} &\theta_1 = P_1\cdot\varphi_1, \qquad \theta_2 = P_2\cdot\varphi_1 + P_1^2\cdot\varphi_2, \qquad \theta_3 = P_3\cdot\varphi_1 + 2P_1\cdot P_2\cdot\varphi_2 + P_1^3\cdot\varphi_3, \\ &S_1 = P_1\cdot\psi_1, \qquad S_2 = P_2\cdot\psi_1 + P_1^2\cdot\psi_2, \qquad S_3 = P_3\cdot\psi_1 + 2P_1\cdot P_2\cdot\psi_2 + P_1^3\cdot\psi_3. \end{aligned} \tag{3.12}$$

Substituting θ_i and S_i $(i = 1, 2, 3)$ into (3.2) and (3.3) yields

$$\theta = P_1\varphi_1\varepsilon + \left(P_2\varphi_1 + P_1^2\varphi_2\right)\varepsilon^2 + \left(P_3\varphi_1 + 2P_1P_2\varphi_2 + P_1^3\varphi_3\right)\varepsilon^3, \tag{3.13}$$

$$S = P_1\psi_1\varepsilon + \left(P_2\psi_1 + P_1^2\psi_2\right)\varepsilon^2 + \left(P_3\psi_1 + 2P_1P_2\psi_2 + P_1^3\psi_3\right)\varepsilon^3. \tag{3.14}$$

In (3.13) and (3.14), the constant coefficients P_i $(i = 1, 2, 3)$ and perturbation parameter ε are unknown quantities. P_i $(i = 1, 2, 3)$ can be determined by giving ε a specific definition according to the traditional perturbation method, but we will not give ε a specific definition in this paper.

4. Spline Function Solution to Functions $\varphi_i(\rho)$ and $\psi_i(\rho)$

Cubic multiple nodes spline function is applied to solve (3.8)–(3.10). Cubic multiple nodes spline function was widely applied to solve nonlinear equations [11].

Transforming (3.8) into integral forms yields

$$\varphi_1(\rho) = -\frac{\rho}{2}\int_0^1 G_1(\rho,\xi)\cdot\xi\cdot u(\xi-\gamma_1)d\xi + \frac{\rho}{2}\cdot\int_0^1 G_1(\rho,\xi)\cdot k\cdot\xi\cdot u(\xi-\gamma_2)\cdot\varphi_1(\xi)d\xi, \tag{4.1}$$

$$\varphi_1(\rho) = -\frac{\rho}{2}\cdot\int_0^1 G_2(\rho,\xi)\cdot k\cdot\xi\cdot u(\xi-\gamma_2)\cdot\varphi_1(\xi)d\xi. \tag{4.2}$$

Substituting (4.2) into (4.1) yields the following nonlinear integral equations:

$$\varphi_1(\rho) = F(\rho) + \int_0^1 K(\rho,\xi)\cdot\varphi_1(\xi)d\xi, \tag{4.3}$$

where

$$F(\rho) = -\frac{\rho}{2}\int_0^1 G_1(\rho,\xi)\cdot\xi\cdot u(\xi-\gamma_1)d\xi, \tag{4.4}$$

$$K(\rho,\xi) = -\frac{1}{4}\int_0^1 k^2\cdot\rho\cdot\xi\cdot\eta^2\cdot u(\eta-\gamma_2)\cdot u(\xi-\gamma_2)\cdot G_1(\rho,\eta)\cdot G_2(\eta,\xi)d\eta, \tag{4.5}$$

$$G_i(\rho,\xi) = \begin{cases} \dfrac{1}{\rho^2}+\lambda_i, & 0<\xi\le\rho \\ \dfrac{1}{\xi^2}+\lambda_i, & \rho<\xi<1 \end{cases} \qquad (i=1,2), \tag{4.6}$$

$$\lambda_1 = \frac{1-\nu_1}{1+\nu_1}, \qquad \lambda_2 = \frac{1+\nu_2}{1-\nu_2}. \tag{4.7}$$

Because $F(\rho)$ and $K(\rho,\xi)$ are continuous on interval $[0,1]$ and square interval $0 \le \rho,\ \xi \le 1$, respectively, the consistent approximation of $F(\rho)$ and $K(\rho,\xi)$ can be obtained by using polynomials on the two intervals.

We make equidistant node division on interval $[0,1]$ and square interval $0 \le \rho,\ \xi \le 1$, the node values are ρ_i and (ρ_i,ξ_i), where $\rho_i = i/N$, $\xi_j = j/M$ $(i = 0,1,\ldots,N; j = 0,1,\ldots,M)$, and N and M are the divided node number.

We use $\widetilde{K}(\rho,\xi)$ and $\widetilde{F}(\rho)$ to replace $F(\rho)$ and $K(\rho,\xi)$ approximately, then the consistent approximation of $F(\rho)$ and $K(\rho,\xi)$ are as follows:

$$\begin{aligned} \widetilde{K}(\rho,\xi) &= \sum_{i=0}^{N}\sum_{j=0}^{M} K_{ij}\times\overset{N}{\phi}_i(\rho)\times\overset{M}{\phi}_j(\xi), \\ \widetilde{F}(\rho) &= \sum_{i=0}^{N} F_i\times\overset{N}{\phi}_i(\rho), \end{aligned} \tag{4.8}$$

where $K_{ij} = K(\rho_i,\xi_j), F_i = F(\rho_i)$, K_{ij}, and F_i denote the function values of corresponding nodes. $\phi_i(\rho)$ and $\phi_j(\xi)$ are cubic multiple nodes spline functions.

Assume that the solution of $\varphi_1(\rho)$ is

$$\varphi_1(\rho) = \sum_{i=0}^{N} \varphi_1(\rho_i) \cdot \phi_i(\rho). \tag{4.9}$$

Substituting (4.8)–(4.9) into (4.3) and making coefficients of $\phi_i(\rho)$ $(i = 0, 1, \ldots, N)$ are equal yields the following linear equations:

$$\varphi_1(\rho_i) - \sum_{k=0}^{N} \varphi_1(\rho_k) \cdot a_{ik} = F_i, \tag{4.10}$$

where

$$\begin{aligned} a_{ik} &= \sum_{j=0}^{M} K_{ij} \cdot c_{jk}, \\ c_{jk} &= \int_0^1 \phi_j(\xi) \cdot \phi_k(\xi) d\xi, \end{aligned} \tag{4.11}$$

$\varphi_1(\rho_\mathrm{i})$ can be obtained by solving linear equations (4.10). Substituting $\varphi_1(\rho_\mathrm{i})$ into (4.9) can obtain an approximate solution of $\varphi_1(\rho)$. We can obtain the approximate solution of (4.2) by using the same method

$$\psi_1(\rho) = \sum_{j=0}^{N} \psi_1(\rho_\mathrm{j}) \cdot \phi_j(\rho). \tag{4.12}$$

Adopting the same method and the data that have been figured out, we also can obtain solutions of (3.9) and (3.10). Therefore, all the approximate solutions of $\varphi_\mathrm{i}(\rho)$ and $\psi_\mathrm{i}(\rho)$ are as follows:

$$\varphi_i(\rho) = \sum_{j=0}^{N} \varphi_i(\rho_j) \cdot \phi_j(\rho), \tag{4.13}$$

$$\psi_i(\rho) = \sum_{j=0}^{N} \psi_i(\rho_j) \cdot \phi_j(\rho). \tag{4.14}$$

5. The Determination of Dimensionless Critical Load and Deflection

5.1. The Determination of Dimensionless Critical Load

Assume that the dimensionless critical load P and deflection W satisfy the following equations:

$$P = \alpha_1(\rho) \cdot W(\rho) + \alpha_2(\rho) \cdot W^2(\rho) + \alpha_3(\rho) \cdot W^3(\rho) + o\left(W^4(\rho)\right), \tag{5.1}$$

$W(\rho)$ can be obtained according to (3.13)

$$W(\rho) = P_1 \cdot Y_1(\rho) \cdot \varepsilon + \left[P_2 \cdot Y_1(\rho) + P_1^2 \cdot Y_2(\rho)\right] \cdot \varepsilon^2 + \left[P_3 \cdot Y_1(\rho) + 2P_1 \cdot P_2 \cdot Y_2(\rho) + P_1^3 \cdot Y_3(\rho)\right] \cdot \varepsilon^3 + o\left(\varepsilon^4\right), \tag{5.2}$$

where

$$Y_i(\rho) = \int_1^\rho \varphi_i(\rho) d\rho \quad (i = 1, 2, 3). \tag{5.3}$$

Substituting (5.2) into (4.1), and omitting high-order minuteness that more than four orders, and comparing with (3.1) yield expressions of $\alpha_i(\rho)$:

$$\begin{aligned} \alpha_1(\rho) &= Y_1^{-1}(\rho), \\ \alpha_2(\rho) &= -Y_1^{-3}(\rho) \cdot Y_2(\rho), \\ \alpha_3(\rho) &= -Y_1^{-4}(\rho) \cdot Y_3(\rho) + 2Y_1^{-5}(\rho) \cdot Y_2^2(\rho). \end{aligned} \tag{5.4}$$

$\varphi_i(\rho)$ $(i = 1, 2, 3)$ can be figured out according to (4.13) and values of $\alpha_i(\rho)$ $(i = 1, 2, 3)$ can be obtained by substituting concrete values of ρ into (5.3) and (5.4). Then, we can obtain the characteristic equation (5.1) that is determined by deflections of different points on shell surface. Therefore, we obtained the solution of (3.13) and (3.14) such as (5.1) while did not determine the perturbation parameter ε. Now, we can calculate the critical geometric parameter k_{cr} and critical load P_{cr} according to the following steps.

Firstly, substituting concrete values of k into extremum condition $dP/dW = 0$ yields

$$W_{\text{cr}} = \frac{\alpha_2 \pm \sqrt{\alpha_2^2 - 3 \cdot \alpha_1 \cdot \alpha_2}}{3 \cdot \alpha_3}. \tag{5.5}$$

The corresponding formula of critical force is

$$P_{\text{cr}} = \alpha_1 \cdot W_{\text{cr}} + \alpha_2 \cdot W_{\text{cr}}^2 + \alpha_3 \cdot W_{\text{cr}}^3. \tag{5.6}$$

For the dished shallow shell whose truncated conical ratio γ and geometric condition k are determined values, each value of ρ have a corresponding group of concrete $\alpha_i(\rho)$ $(i = 1, 2, 3)$. Then we can find values of k that satisfy the following condition according to trial method.

$$\alpha_2^2 - 3\alpha_1 \cdot \alpha_3 = 0. \tag{5.7}$$

Here, k, namely (5.6), is significant. That is, only $k \geq k_{\text{cr}}$ with (5.6) is significant, and the instability phenomenon is existent, namely, the jumping phenomenon of dished shallow shell happen.

Comparing all corresponding critical loads of values of ρ, the minimum critical load is the critical load for initial instability.

5.2. The Determination of Deflection of Each Point under Dimensionless Loads

For the dished shallow shell whose truncated conical ratio γ and geometric condition k are determined values, the elastic characteristic equation of dimensionless load and deflection (5.1) is permanently significant when P is equal or less than the initial instability critical load.

For the dished shallow shell whose geometric condition is k, each value of ρ has a corresponding group of concrete $\alpha_i(\rho)$ $(i = 1, 2, 3)$. Then, we can construct a concrete function P with respect to $W(\rho)$.

From the analysis of (5.1), we know that for concrete value of ρ, $\alpha_i(\rho)$ $(i = 1, 2, 3)$ is a determined value. Here, if P is a determined value, (5.1) is a standard simple cubic equation. Therefore, we can obtain the deflection value $W(\rho)$ according to the solving method of simple cubic equations supplied in paper [11]. That is, we can get the deflection of each point when the external load is determined.

If we figure out the deflection of each point when the geometric condition is k and the external load is initial instability critical load, we can determine the corresponding initial instability mode of the dished shallow shell under determined geometric condition and initial instability critical load.

If we figure out the deflection of each point under corresponding external load when the geometric condition is k and the external load equal or less than the initial instability critical load, we can obtain the deflection curve of the dished shallow shell under specific geometric condition and external load.

6. Computational Examples and Analysis of Numerical Results

In the following computational example, the number of fitting point is $M = N = 100$ and the Poisson's ratio is $v = 0.3$.

For the dished shallow shell under circular line load p' whose boundary condition is simply supported, we take $\gamma = 0.3$ and $\gamma' = 0.2,\ 0.3,\ 0.5$, then $v_1 = 0.3$, $v_2 = 0.3$. We can figure out $\lambda_1 = 0.538461$, $\lambda_2 = 1.857143$ according to (4.7).

The characteristic equation (5.1) constructed by deflection of arbitrary point is

$$P = \alpha_1(\rho) \cdot W(\rho) + \alpha_2(\rho) \cdot W^2(\rho) + \alpha_3(\rho) \cdot W^3(\rho). \tag{6.1}$$

The corresponding $P_{cr} - \rho$ curves of different values of k are shown in Figures 2(a), 3(a), and 4(a) while truncated conical ratio $\gamma = 0.3$ and $\gamma' = 0.2,\ 0.3,\ 0.5$, respectively. The abscissa value denotes the radius value of the pint, where the perturbation parameter is selected and the ordinate value denotes the corresponding value of critical load in Figures 2(a), 3(a), and 4(a). The abscissa value of the lowest point of P_{cr}-ρ curve is the radius value of initial instability point of dished shallow shell. The ordinate value of the lowest point of P_{cr}-ρ curve is the initial instability critical load of dished shallow shell.

The corresponding $W(\rho)$-ρ curves of different values of k are shown in Figures 2(b), 3(b), and 4(b), while P increase progressively and truncated conical ratio $\gamma = 0.3$ and

$\gamma' = 0.2,\ 0.3,\ 0.5$, respectively. The abscissa value denotes the radius value of the pint, where the perturbation parameter is selected and the ordinate value denotes the dimensionless deflection value in Figures 2(b), 3(b), and 4(b). The abscissa value of the highest point of $W(\rho) - \rho$ curve is the radius value of the largest deflection point of dished shallow shell. The corresponding $W(\rho) - \rho$ curve is the initial instability mode when P is initial instability critical load.

In order to explain Figures 2(a) and 2(b), we listed the initial instability and maximum deflection position of the dished shallow shell under different geometric parameters in Table 1.

We can obtain the following conclusions from Figures 2(a) and 2(b) and Table 1.

(1) When the circular line load acted on the circular plate section, the initial instability area of dished shallow shell moved from the center of circular plate to the edge of dished shallow shell with the increase of k while $3 \leq k \leq 7$. The initial instability area of dished shallow shell moved from the edge of dished shallow shell to the edge of circular plate with the increase of k while $k > 7$.

(2) With the stepwise increase of external load, the increase amplitude of deflection of each point enlarged, but the area of maximum deflection almost did not move, and the deflection where the circular line load acted on did not fluctuate markedly. The maximum deflection area of dished shallow shell under external load appeared at the center of circular plate ($\rho = 0$) while $k \geq 3$.

(3) When the external load got close to the initial instability critical load, the increase amplitude of deflection of each point near the initial instability area was significant. The maximum deflection area of initial instability appeared at the center of circular plate ($\rho = 0$) while $k \geq 3$.

As the supplementary specification data for Figures 3(a) and 3(b), the initial instability and maximum deflection position of the dished shallow shell under different geometric parameters are listed in Table 2.

We can obtain the following conclusions from Figures 3(a) and 3(b) and Table 2.

(1) When the circular line load acted on the edge of circular plate, the initial instability area of dished shallow shell moved from the loading action position to the edge of dished shallow shell with the increase of k while $4 \leq k \leq 7$, and the initial instability area of dished shallow shell moved from the edge of dished shallow shell to the center of circular plate with the increase of k while $k > 7$.

(2) With the stepwise increase of external load, the increase amplitude of deflection of each point was enlarged, but the maximum deflection area almost did not move, and the deflection where the circular line load acted on did not fluctuate markedly. The maximum deflection area of dished shallow shell under external load appeared at the center of circular plate ($\rho = 0$) while $k \geq 4$.

(3) When the external load got close to the initial instability critical load, the increase amplitude of deflection of each point near the initial instability area was significant. The maximum deflection area of initial instability appeared at the center of circular plate ($\rho = 0$) while $k \geq 4$.

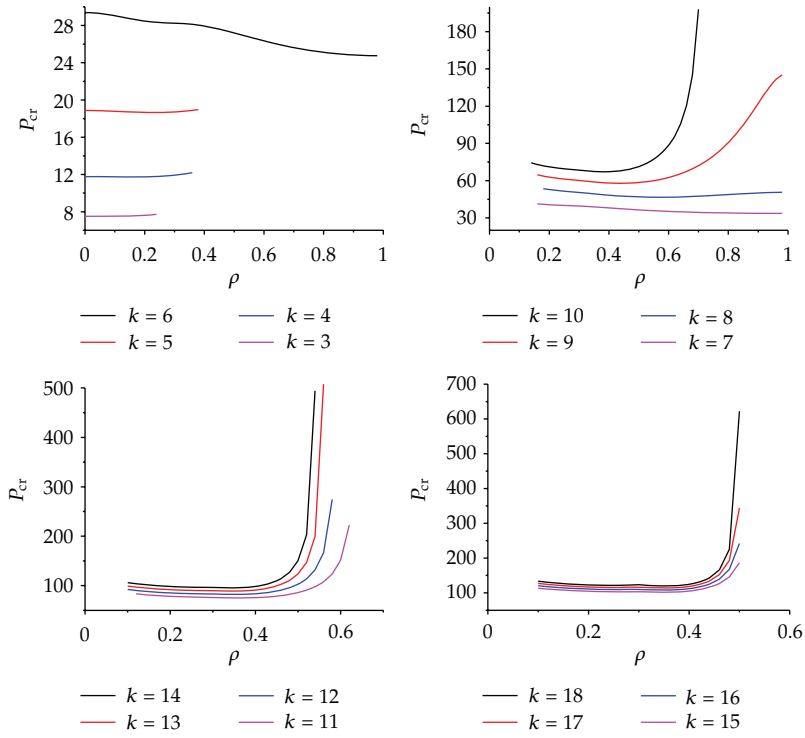

(a) P_{cr}-ρ curves ($\gamma = 0.3$, $\gamma' = 0.2$)

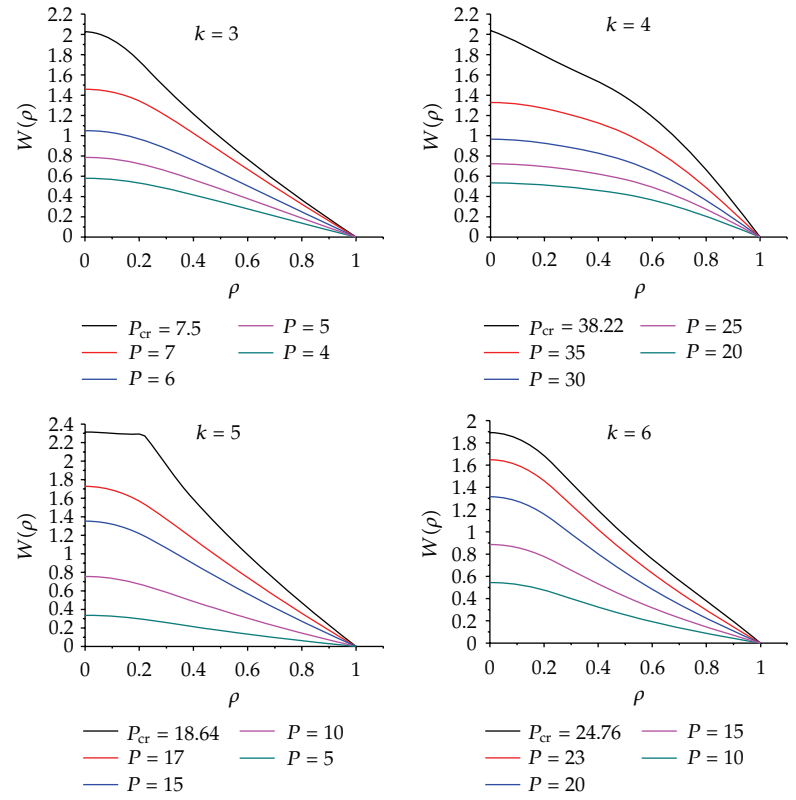

(b)

Figure 2: Continued.

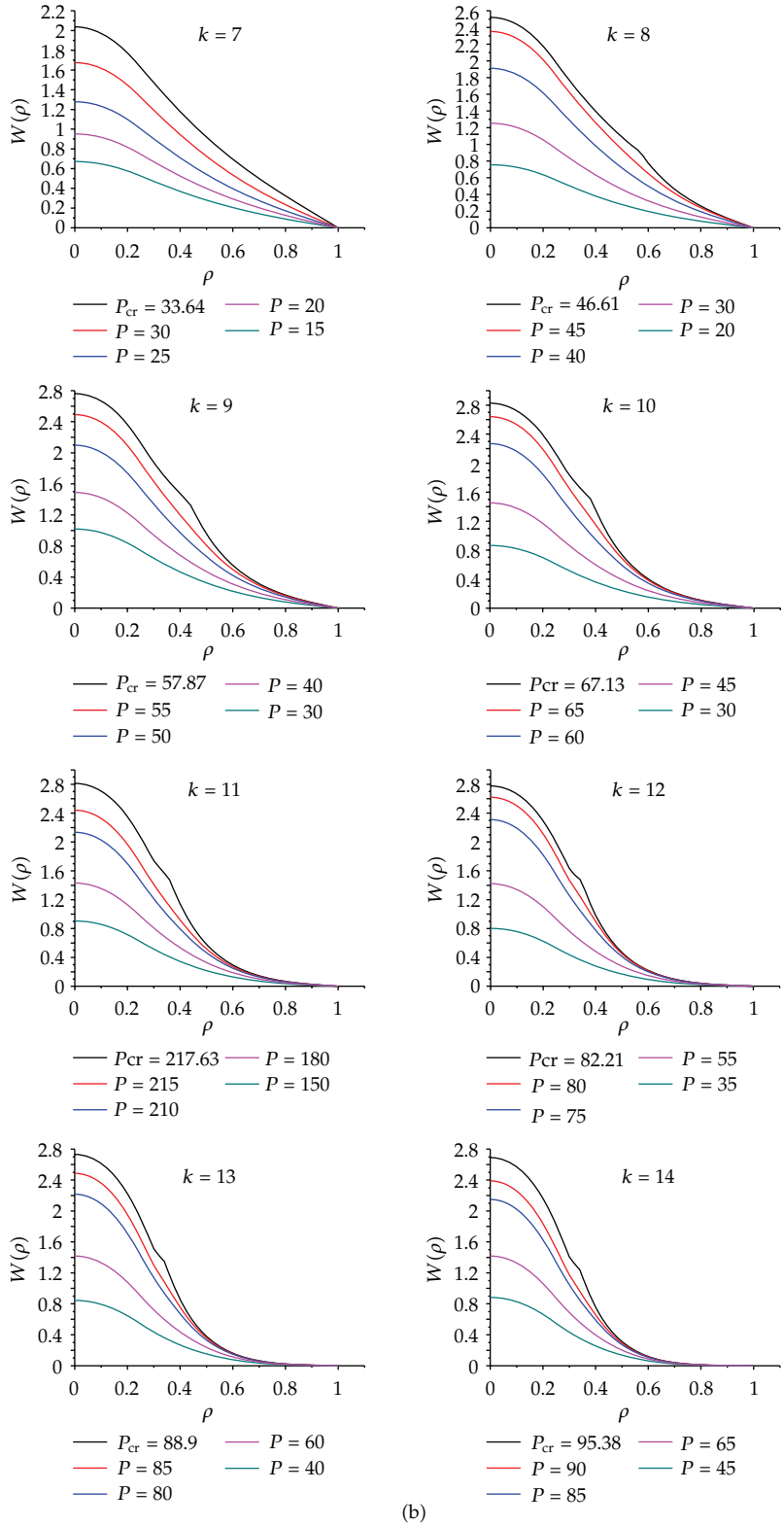

(b)

Figure 2: Continued.

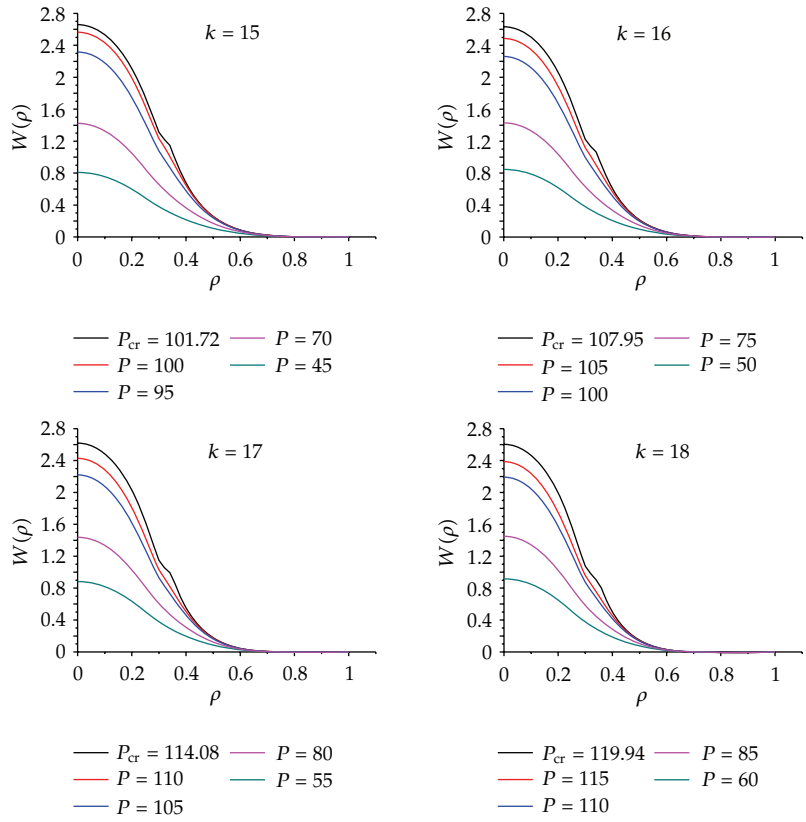

(b) $W(\rho)$-ρ curves ($\gamma = 0.3$, $\gamma' = 0.2$)

Figure 2

Table 1: The initial instability and maximum deflection position under different geometric parameters ($\gamma = 0.3, \gamma' = 0.2$).

The geometric parameter: k =	3	4	5	6	7	8	9	10
The initial instability position: ρ =	0.00	0.16	0.22	0.98	0.99	0.56	0.44	0.38
The maximum deflection position: ρ =	0.00	0.00	0.00	0.00	0.00	0.00	0.00	0.00
The geometric parameter: k =	11	12	13	14	15	16	17	18
The initial instability position: ρ =	0.36	0.34	0.34	0.34	0.34	0.34	0.34	0.34
The maximum deflection position: ρ =	0.00	0.00	0.00	0.00	0.00	0.00	0.00	0.00

Likewise, in order to explain Figures 4(a) and 4(b), we listed the initial instability and maximum deflection position of the dished shallow shell under different geometric parameters in Table 3.

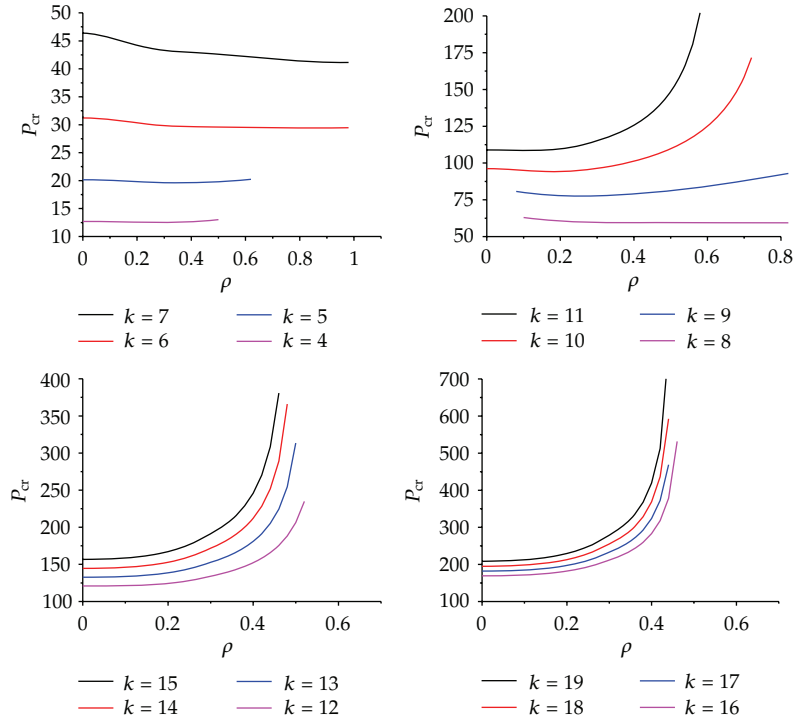

(a): P_{cr}-ρ curves ($\gamma = 0.3$, $\gamma' = 0.3$)

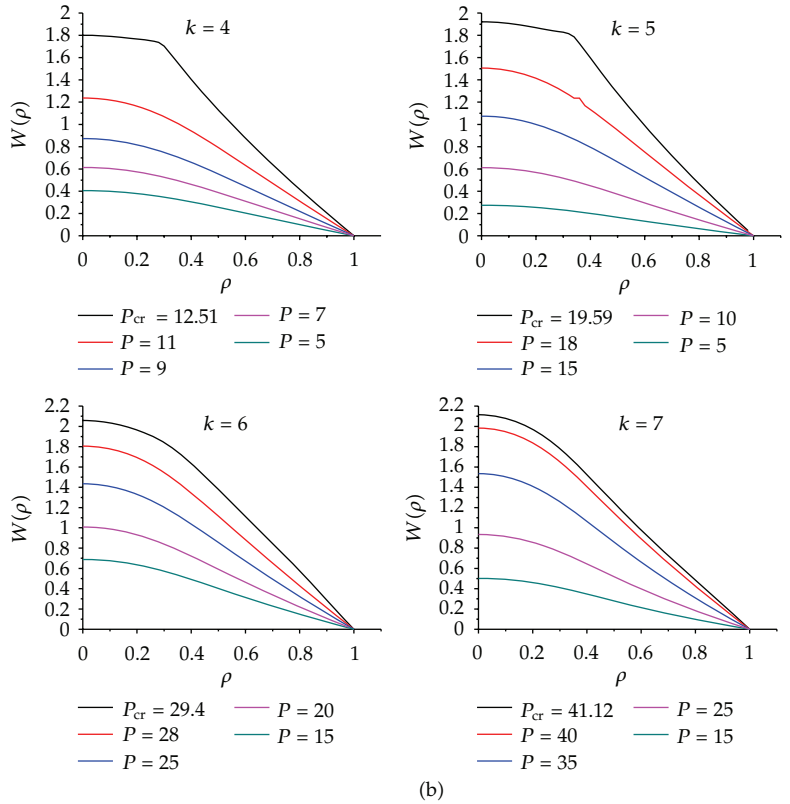

(b)

Figure 3: Continued.

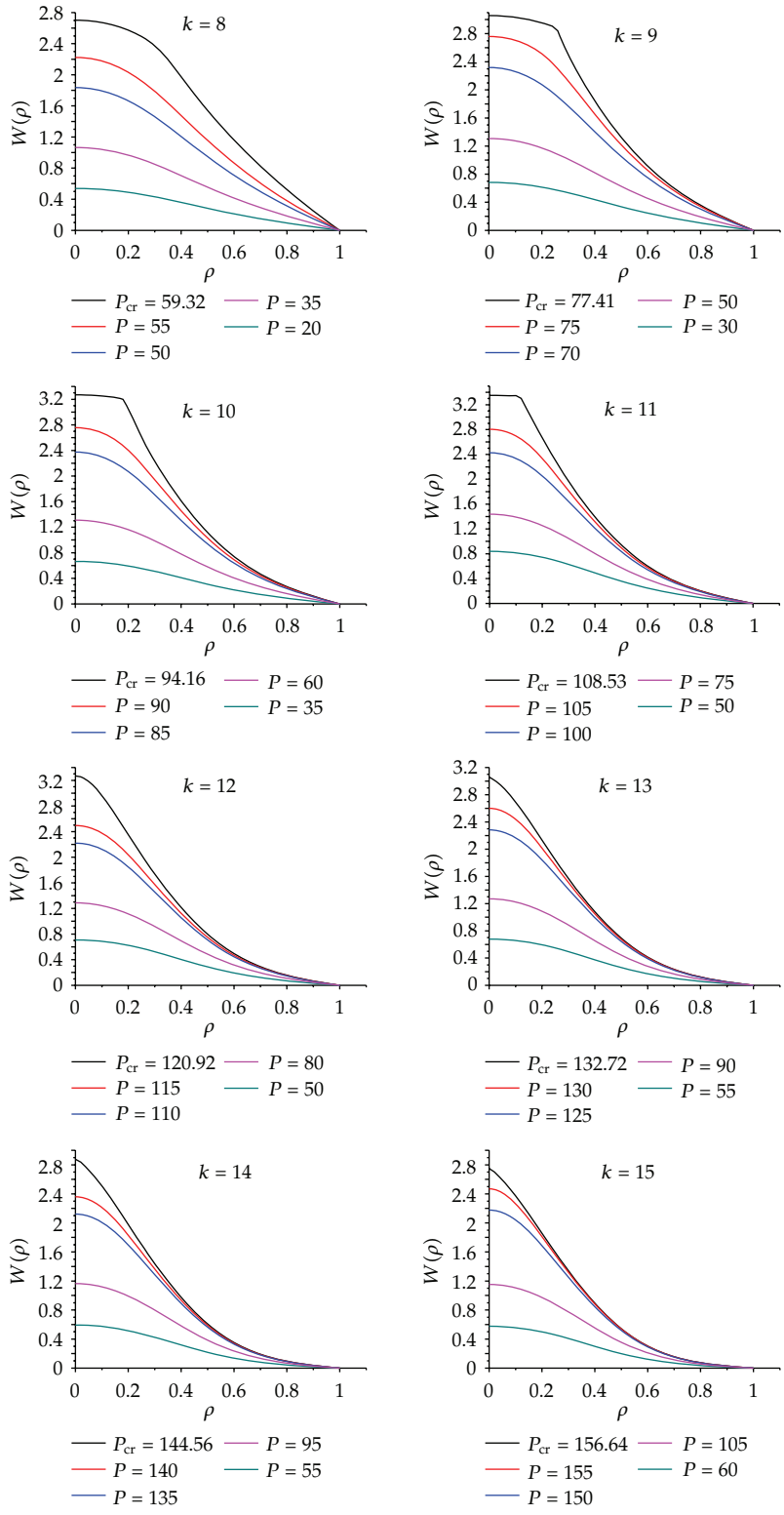

(b)

Figure 3: Continued.

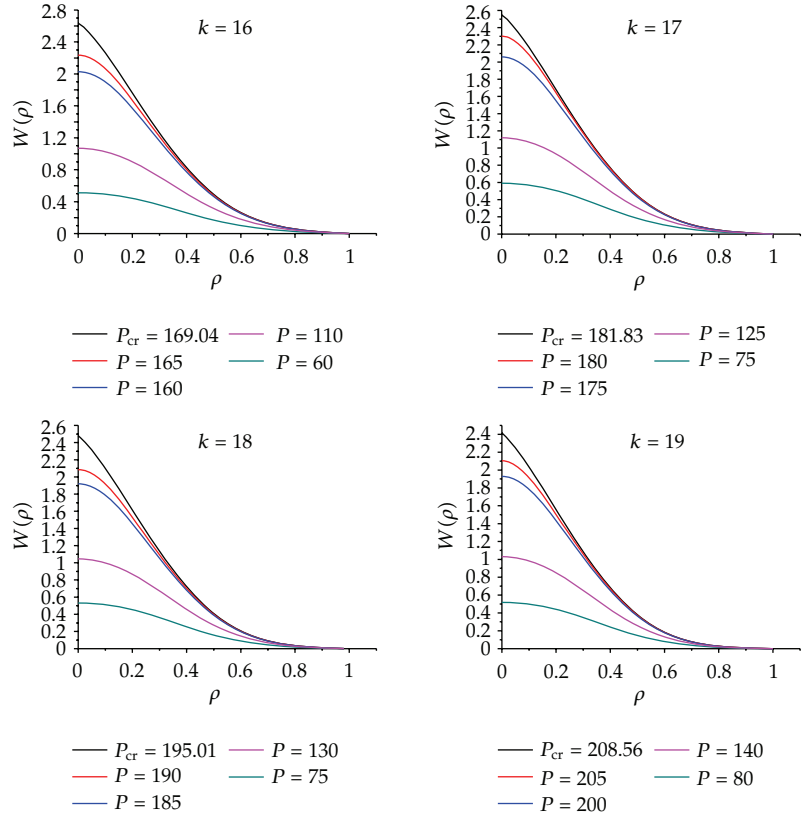

(b) $W(\rho)$-ρ curves ($\gamma = 0.3$, $\gamma' = 0.3$)

Figure 3

We can obtain the following conclusions from Figures 4(a) and 4(b) and Table 3.

(1) When the circular line load acted on the conical shell section, the initial instability area moved from the loading action position to the center of circular plate with the increase of k while $4 \leq k \leq 7$; the initial instability area appeared at the center of circular plate while $7 \leq k \leq 9$; the initial instability area moved from the center to the edge of circular plate with the increase of k while $9 < k \leq 12$; the initial instability area moved from the edge to the center of circular plate with the increase of k while $k > 12$.

(2) With the stepwise increase of external load, the increase amplitude of deflection of each point was enlarged, but the maximum deflection area under each step load almost did not move. The maximum deflection area of dished shallow shell under external load appeared at the center of circular plate ($\rho = 0$) while $4 \leq k < 7$, and the maximum deflection area appeared at the loading action position while $k \geq 7$.

(3) When the external load was close to the initial instability critical load, the increase amplitude of deflection of each point near the initial instability area was significant. The maximum deflection area of initial instability appeared at the center of circular plate ($\rho = 0$) while $4 \leq k \leq 5$ and $6 < k \leq 8$; the maximum deflection area appeared at the loading action position and its adjacent area while $5 < k \leq 6$ and $k > 8$.

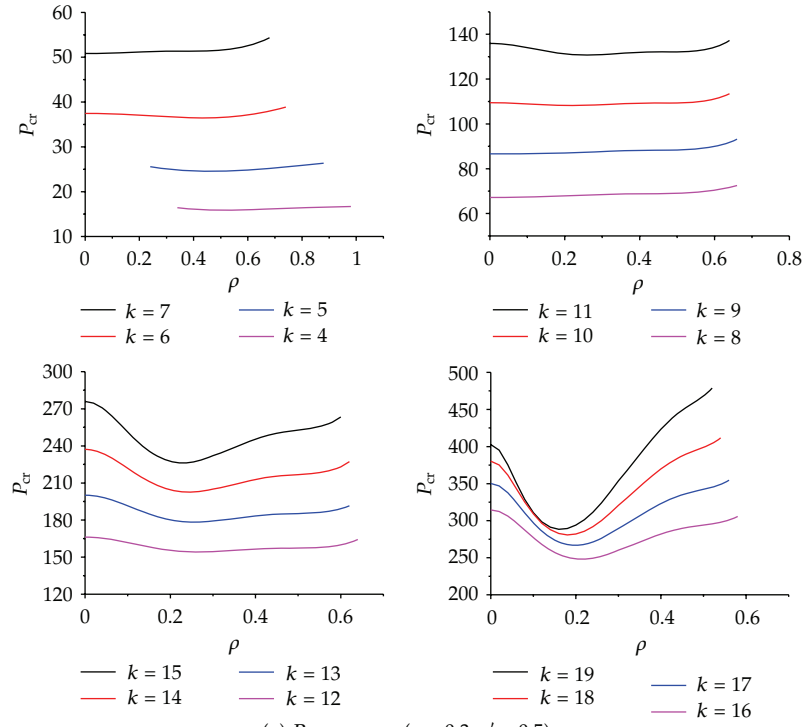

(a) P_{cr}-ρ curves ($\gamma = 0.3$, $\gamma' = 0.5$)

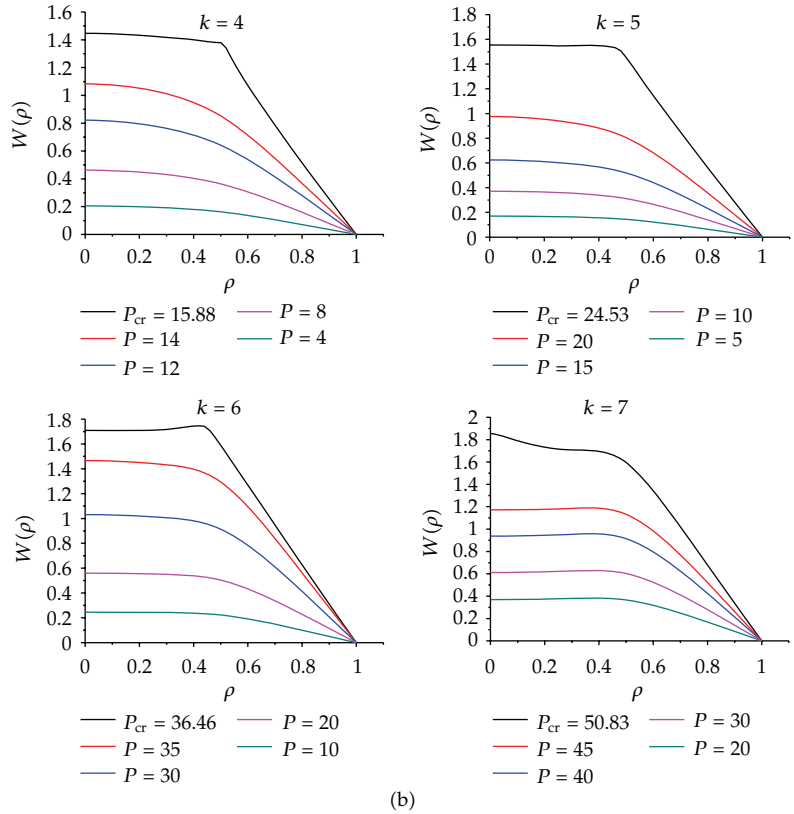

(b)

Figure 4: Continued.

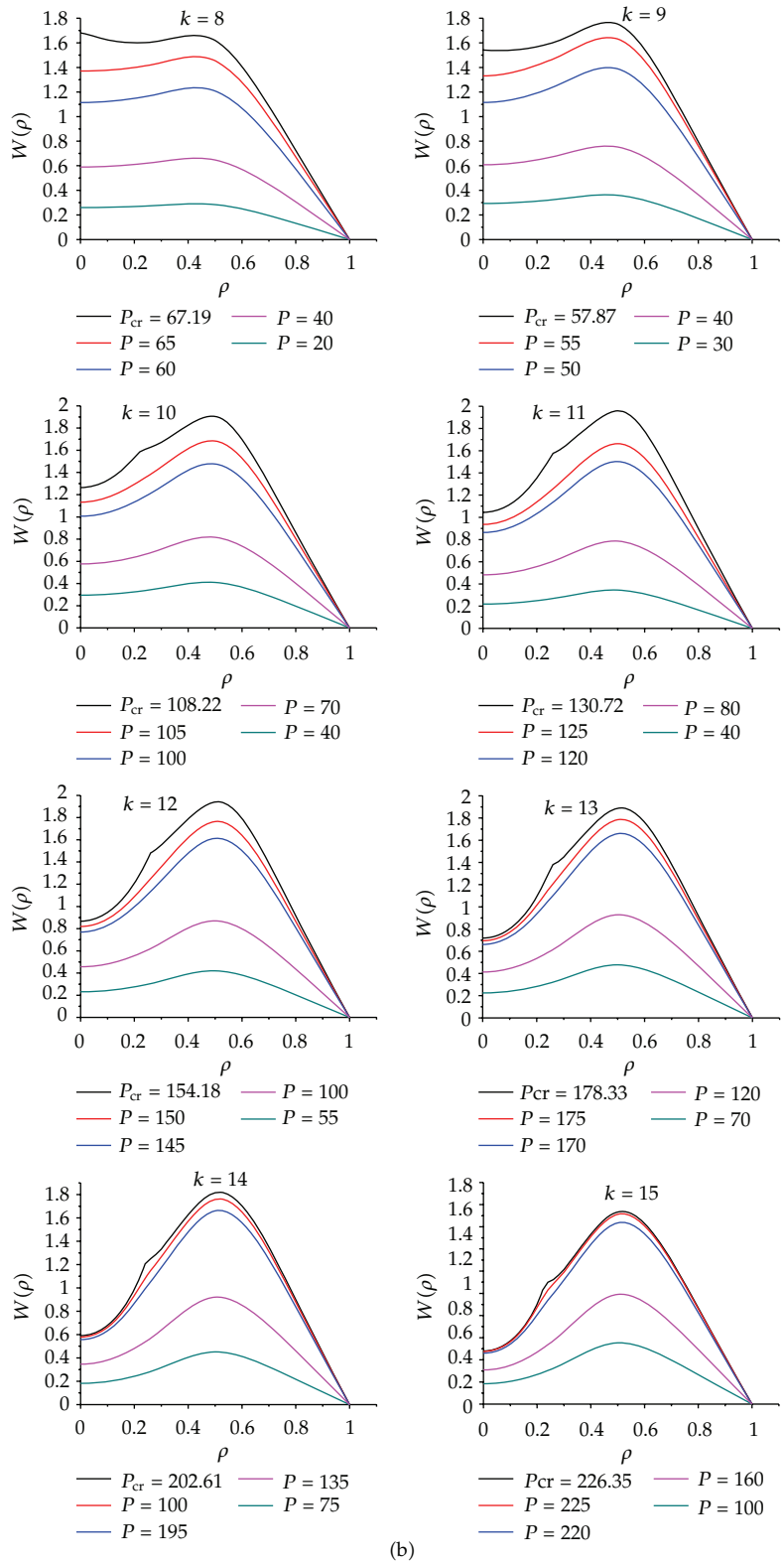

(b)

Figure 4: Continued.

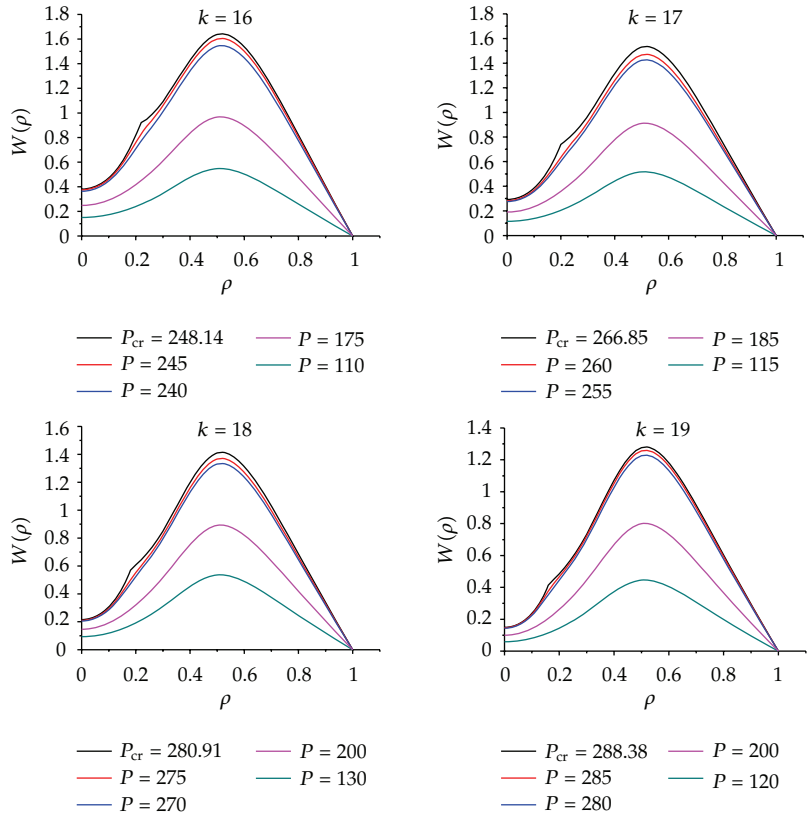

(b) $W(\rho)$-ρ curves ($\gamma = 0.3$, $\gamma' = 0.5$)

Figure 4

Table 2: The initial instability and maximum deflection position under different geometric parameters ($\gamma = 0.3, \gamma' = 0.3$).

The geometric parameter: k =	4	5	6	7	8	9	10	11
The initial instability position: ρ =	0.30	0.34	0.86	0.98	0.80	0.26	0.18	0.12
The maximum deflection position: ρ =	0.00	0.00	0.00	0.00	0.00	0.00	0.00	0.00
The geometric parameter: k =	12	13	14	15	16	17	18	19
The initial instability position: ρ =	0.00	0.00	0.00	0.00	0.00	0.00	0.00	0.00
The maximum deflection position: ρ =	0.00	0.00	0.00	0.00	0.00	0.00	0.00	0.00

7. Conclusions

This paper obtained the nonlinear instability modes of dished shallow shell under circular line load by applying free-parameter perturbation method. By analyzing the nonlinear instability modes, we obtained the following conclusions.

Table 3: The initial instability and maximum deflection position under different geometric parameters ($\gamma = 0.3, \gamma' = 0.5$).

The geometric parameter: k =	4	5	6	7	8	9	10	11
The initial instability position: ρ =	0.50	0.48	0.44	0.00	0.00	0.00	0.22	0.26
The maximum deflection position: ρ =	0.00	0.00	0.42	0.00	0.00	0.46	0.48	0.50
The geometric parameter: k =	12	13	14	15	16	17	18	19
The initial instability position: ρ =	0.28	0.26	0.24	0.22	0.20	0.18	0.16	0.14
The maximum deflection position: ρ =	0.50	0.52	0.52	0.52	0.52	0.52	0.52	0.52

(1) When the circular line load act on the circular plate, the edge of circular plate, and the conical shell, respectively, and the geometric parameter k is relatively small, the initial instability area of dished shallow shell appears at the loading action position, but the maximum deflection area of initial instability appear at the center of circular plate ($\rho = 0$).

(2) The initial instability area of dished shallow shell under circular line load does not always appear at the loading action position. The initial instability area of dished shallow with different γ and γ' presents different rules with the variation of k when k is relatively large. The maximum deflection area of initial instability appears at the center of circular plate ($\rho = 0$) when the circular line load act on the circular plate, the edge of circular plate, and the conical shell, respectively. The maximum deflection area of initial instability appears at the loading action position when the circular line load act on the conical shell and k is relatively large.

(3) With the stepwise increase of external load, the increase amplitude of deflection of each point of dished shallow shell was enlarged. Under each step load, the maximum deflection area of dished shallow shell almost does not move, and the deflection where the circular line load act on does not fluctuate markedly, but the maximum deflection area of initial instability will move from its lateral side to itself when the circular line load act on the conical shell and γ is relatively large. The increase amplitude of deflection of each point near the initial instability area is significant when the external load is close to the initial instability critical load.

(4) The maximum deflection area of dished shallow shell presents different rules with the variation of k, γ, and γ'. But, when the external load gets close to the initial instability critical load, the increase amplitude of deflection of each point near the initial instability area is significant, so the maximum deflection area of initial instability is not always the maximum deflection area under the previous load.

(5) When the geometric parameter k is a determined value, the critical load when the circular line load act on the conical shell is larger than the critical load when the circular line load act on the circular plate and the edge of circular plate, but the maximum deflection of initial instability when the circular line load act on the conical shell is smaller than the maximum deflection of initial instability when the circular line load act on the circular plate and the edge of circular plate. That is, the critical load increase with the increase of γ', but the maximum deflection of initial instability decrease with the increase of γ'.

These conclusions provide some theoretical basis for engineering design and instability prediction and control of shallow-shell structures.

Acknowledgment

This work has been supported by the Science and Technology Program of Chongqing Municipal Education Commission: Free-Parameter Perturbation Method (Project no. KJ08A12).

References

[1] D. Liu and S.-L. Chen, "Snap-buckling of dished shallow shells under uniform loads," *Applied Mathematics and Mechanics*, vol. 18, no. 1, pp. 29–36, 1997.
[2] D. Liu and S.-L. Chen, "Snap-buckling of dished shallow shells under line loads," *Applied Mathematics and Mechanics*, vol. 19, no. 3, pp. 227–234, 1998.
[3] A. Chakrabarti, B. Mukhopadhyay, and R. K. Bera, "Nonlinear stability of a shallow unsymmetrical heated orthotropic sandwich shell of double curvature with orthotropic core," *International Journal of Solids and Structures*, vol. 44, no. 16, pp. 5412–5424, 2007.
[4] J. Tani, "Buckling of truncated conical shells under combined axial load, pressure, and heating," *Journal of Applied Mechanics, Transactions ASME*, vol. 52, no. 2, pp. 402–408, 1985.
[5] J.-C. Xu, C. Wang, and R.-H. Liu, "Nonlinear stability of truncated shallow conical sandwich shell with variable thickness," *Applied Mathematics and Mechanics*, vol. 21, no. 9, pp. 985–986, 2000.
[6] H. Ramsey, "Plastic buckling of conical shells under axial compression," *International Journal of Mechanical Sciences*, vol. 19, no. 5, pp. 257–258, 1977.
[7] H. Wang and J.-K. Wang, "Snap-buckling of thin shallow conical shells," *Engineering Mechanics*, vol. 7, no. 1, pp. 27–33, 1990.
[8] Z.-L. Zheng, B.-Q. Sun, B. Li, and S.-L. Chen, "Nonlinear local stability of dished shallow shells under uniformly distributed loads," *Journal of Chongqing University*, vol. 30, no. 12, pp. 55–58, 2007.
[9] S.-L. Chen and Q.-Z. Li, "Free-parameter perturbation-method solutions of the nonlinear stability of shallow spherical shells," *Applied Mathematics and Mechanics*, vol. 25, no. 9, pp. 881–888, 2004.
[10] S.-L. Chen, "Free-parameter perturbation method," in *A festschrift for the 90th birthday of Professor W.-Z. Chien*, Z.-W. Zhou, Ed., pp. 35–43, Shanghai University Press, Shanghai, China, 2003.
[11] K.-Y. Ye and W.-P. Song, "Deformations and stability of spherical caps under centrally distributed pressures," *Applied Mathematics and Mechanics*, vol. 9, no. 10, pp. 857–863, 1988.